Symmetry breaking in the body-fixed electron emission pattern due to electron-retroaction in the photodissociation of H_2^+ and D_2^+ close to threshold

S. Heck,[1,2,3] A. Gatton,[1,4] K. A. Larsen,[1,5] W. Iskandar,[1] E. G. Champenois,[1] R. Strom,[4] A. Landers,[4] D. Reedy,[6] C. Dailey,[6] J. B. Williams,[6] T. Severt,[7] B. Jochim,[7] I. Ben-Itzhak,[7] R. Moshammer,[2] R. Dörner,[3] D. S. Slaughter,[1] and Th. Weber[1]

[1]*Chemical Sciences Division, Lawrence Berkeley National Laboratory, Berkeley, California 94720, USA*

[2]*Max-Planck-Institut für Kernphysik, Saupfercheckweg 1, 69117 Heidelberg, Germany*

[3]*Institut für Kernphysik, J.W. Goethe Universität, Max-von-Laue-Strasse 1, 60438 Frankfurt, Germany*

[4]*Department of Physics, Auburn University, Auburn, Alabama 36849, USA*

[5]*Graduate Group of Applied Science and Technology, University of California, Berkeley, California 94720, USA*

[6]*Department of Physics, University of Nevada Reno, Reno, Nevada 89557, USA*

[7]*J. R. Macdonald Laboratory, Department of Physics, Kansas State University, Manhattan, Kansas 66506, USA*

(Received 7 August 2019; published 3 December 2019)

We present an experimental investigation of symmetry breaking of H_2 and D_2 molecules after single photoionization due to the Coulomb field of the emitted slow electron interacting with the parent cation during dissociation. The experiments were carried out by measuring the three-dimensional momentum vectors of the photoelectron and recoiling ion in coincidence using a reaction microscope. For photon energies close to threshold, the low-energy photoelectron influences the dissociation process, which results in an asymmetric molecular frame photoelectron angular distribution. This can be explained by the retroaction of the Coulomb field of the photoelectron on its parent ion and has been recently experimentally demonstrated by M. Waitz *et al.* [Phys. Rev. Lett. **116**, 043001 (2016)], confirming theoretical predictions by V. V. Serov and A. S. Kheifets [Phys. Rev. A **89**, 031402(R) (2014)]. High-momentum resolution and a new series of photon energies just above the dissociation threshold enable the observation of a strong influence of the electron energy and nuclear kinetic energy on the electron localization process for energies below ∼100 meV, which so far has neither been observed nor discussed by theory. Exploring the limitations of the retroaction mechanism at our lowest photon energy, we are able to single out a sensitive testbed and present data of non-Born-Oppenheimer dynamics of the simplest molecular system for future benchmark computational treatments.

DOI: 10.1103/PhysRevResearch.1.033140

I. INTRODUCTION

Symmetry is an important property of atoms and molecules in photoionization processes. It sets strict rules for the emission patterns of electrons with respect to any distinguishable axis, such as the direction of the light polarization vector or the molecular orientation. In homonuclear molecules, symmetry restrictions allow the electronic eigenfunction to have either gerade or ungerade parity. Consequently, for the photoionization with subsequent dissociation of homonuclear diatomic molecules, the perfect symmetry of the electronic wave functions leads to an equal probability for creating a hole at either one of the two fragments.

There are, however, several possibilities to break this intrinsic symmetry of a homonuclear molecule such as H_2. The most straightforward way to actively do so is by coupling gerade and ungerade wave functions of energetically degenerate final target states via an external field. The superposition of gerade and ungerade contributions then results in an asymmetric photoelectron angular distribution or, in other words, this asymmetric electron emission pattern stems from a localization of the remaining bound electron at a particular nuclear fragment. There have been several experiments in recent years utilizing a strong laser field to induce symmetry breakdown in the dissociation of H_2 molecules [1–7].

Symmetry breaking via superposition of states with gerade and ungerade symmetry can also be achieved without external fields. In the photodissociation of H_2 molecules with linearly polarized light, the coherent superposition of gerade and ungerade electronic states, caused by autoionization, leads to an asymmetric photoelectron emission pattern that is highly sensitive to the kinetic energies of the electron and recoiling nuclear fragments. Full quantum calculations are able to describe this process very accurately [8]. It is conceivable that they can provide the starting point for an accurate theoretical description of a new way of symmetry breaking and beyond, as reflected on later in this paper.

In this paper we focus on a recently discovered fundamental way to coherently mix states of gerade and ungerade parity, using an internal field. In this scenario we lower the photon energy toward the threshold of dissociation, creating ever

slower photoelectrons in a series of measurements. For such low-energy photoelectrons, the Coulomb field of the outgoing electron, scaling as $1/r$, is strong enough to couple the $1s\sigma_g$ and $2p\sigma_u$ states of the parent ion and break the symmetry in the direction to which the bound electron localizes via retroaction. The term "retroaction" for this post-ionization interaction is used to stress the point that the slowly departing photoelectron still influences the left behind molecular ion during its dissociation process. At the limit of this special ionization process, a recapture of the electron can occur, preventing the dissociation of the parent molecular cation to take place. In this paper we again study the retroaction process in the photodissociation of H_2 and D_2 molecules, in order to shine more light on its sensitivity to the kinetic energies of the free particles and the coupling of electron and nuclear dynamics during the dissociation, which is of particular relevance when light atoms such as hydrogen are involved [9,10].

II. EXPERIMENTAL APPROACH

To investigate electron-retroaction in high detail, we conducted several photoionization measurements on H_2 molecules, with photon energies of 19.8, 18.5, 18.3, and 18.16 eV, and on D_2 molecules with an energy of 18.5 eV. The measurements were carried out with monochromatic linearly polarized VUV light at the undulator beamline 10.0.1 of the Advanced Light Source (ALS) synchrotron facility, located at Lawrence Berkeley National Laboratory. The energy offset of the monochromator of the beamline was determined with photoeffect measurements on helium atoms to be $\leqslant$50 meV. The photon energy resolution was $\leqslant$15 meV. A vibrationally cold H_2 or D_2 molecular beam (temperature $\sim$80 K) was produced via a supersonic expansion through a 50-μm nozzle and two skimmers, collimating the beam laterally. The photon and target beams were crossed inside a three-dimensional (3D) momentum imaging spectrometer at right angle, resulting in photoionization events with a rate of less than one event per shot. For each single-ionization event the charged particles, i.e., one electron and one ion, were detected in coincidence with 4π solid angle, using the COLd Target Recoil Ion Momentum Spectroscopy (COLTRIMS) technique [11,12]. The expected heavy reaction products can either be a parent ion H_2^+ (nondissociative ionization) or a proton H^+ and a hydrogen atom H (dissociative ionization).

Exploiting momentum conservation, it is straightforward to determine the momentum vector of the neutral fragment of the dissociation H, as long as all other charged particles, i.e., the electron and proton, are detected. In general, due to the very low photon energies, the photoelectron energy E_e, and hence the momentum of the electron, is small compared to the momenta of the molecular fragments. Here, we are interested in small changes at low nuclear kinetic energies, and therefore it is necessary to correct for the electron momentum transfer onto the molecule during the ionization process. As noted in Ref. [13], this is achieved by calculating

$$\vec{k}_p^{\,\mathrm{c.m.}} \simeq \vec{k}_p^{\,\mathrm{lab}} + 0.5 \cdot \vec{k}_e^{\,\mathrm{lab}}, \tag{1}$$

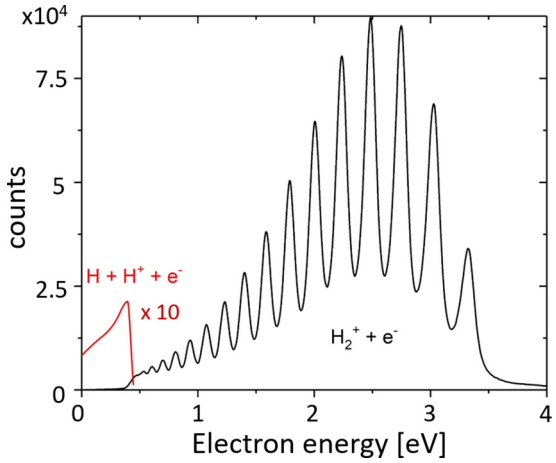

FIG. 1. Measured electron energy distribution for the nondissociative channel (black line) and for the dissociative channel (red line) in the single ionization of H_2 molecules with a photon energy of 18.5 eV. The counts from the dissociative channel are multiplied by 10 to allow for comparison.

where $\vec{k}_p^{\,\mathrm{c.m.}}$ and $\vec{k}_p^{\,\mathrm{lab}}$ are the proton momentum in the H_2^+ center-of-mass frame and the laboratory frame, respectively; accordingly, $\vec{k}_e^{\,\mathrm{lab}}$ is the electron momentum in the laboratory frame.

III. PHOTOELECTRON ENERGY

Our highly differential electron-ion coincidence method allows the complete separation of the predominant nondissociative photoionization channel:

$$H_2 + h\nu \rightarrow H_2^+ + e^- \tag{2}$$

from the dissociative channel:

$$H_2 + h\nu \rightarrow H^+ + H + e^-. \tag{3}$$

Figure 1 shows the kinetic energy distributions of the collected photoelectrons E_e of these two channels. The black line corresponds to the nondissociative single-ionization channel, and the sharp peaks represent the different vibrational levels of the H_2^+ final state. The full width at half maximum (FWHM) of those peaks are a good measure of our electron energy resolution, which was on average $\leqslant$100 meV. The red line in the lower left corner originates from the dissociative ionization. We focus on this faint channel throughout the remainder of this paper.

IV. ENERGY CORRELATION MAPS

The dissociative single-ionization threshold for H_2 molecules is $E_{\mathrm{diss}}(H_2) = 18.078$ eV [9] [$E_{\mathrm{diss}}(D_2) = 18.158$ eV [14]] and the remaining kinetic energy $E_{\mathrm{sum}} = h\nu - E_{\mathrm{diss}}$ is shared between the nuclei and electron. The distribution of this constant sum energy E_{sum} between the nuclei and electron can be seen in Fig. 2 for all photon energies measured in the molecular hydrogen case. In those two-dimensional (2D) energy correlation maps we plot the yield of the dissociative channel as a function of the kinetic energy of the photoelectron (E_e) and the kinetic energy

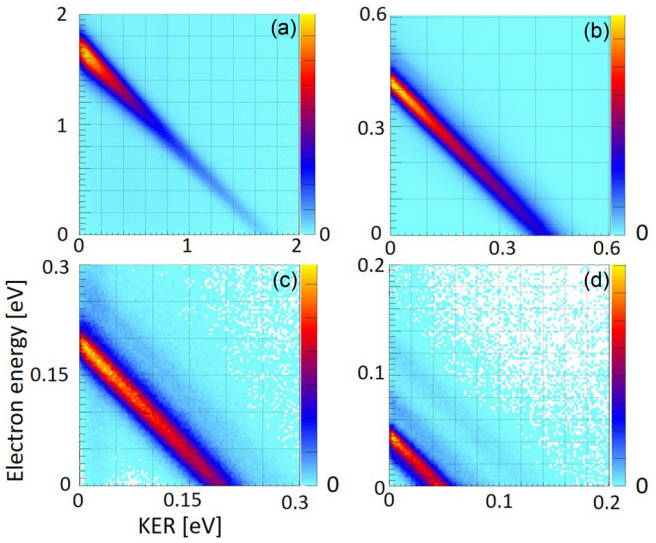

FIG. 2. Energy correlation map between the electron energy E_e and the kinetic energy release KER in the H_2^+ dissociation channel for photon energies of 19.8 eV (a), 18.5 eV (b), 18.3 eV (c), and 18.16 eV (d). The yield is given as a linear color scale in arbitrary units. Note: The yields in the panels are not internormalized to each other.

release (KER) of the nuclei. The diagonal structures represent the constant sum energy

$$E_{\text{sum}} = \text{KER} + E_e = h\nu - E_{\text{diss}}, \tag{4}$$

which arises due to conservation of energy. The width of these distributions is determined by the resolution of our spectrometer, which is strongly dependent on the magnitude of the electromagnetic extraction fields. We optimized these parameters for each photon energy to achieve highest possible energy resolution and attained values ranging from 20 meV for 18.16-eV photon energy to 200 meV for 19.8-eV photon energy.

As can be seen in Figs. 2(c) and 2(d), for the two lowest photon energies 18.3 and 18.16 eV, the energy resolution is high enough to resolve the initial rotationally excited states of orthohydrogen and parahydrogen. They show up as faint parallel diagonals with slightly different sum energy. For example, for a photon energy of 18.16 eV in Fig. 2(d) we find $E_{\text{sum}} = 34$, 45, 75, and 125 meV.

V. MOLECULAR FRAME PHOTOELECTRON ANGULAR DISTRIBUTION (MFPAD)

Plotting the angle between the molecular axis represented by $\vec{k}_p^{\text{c.m.}}$ and the photoelectron momentum vector allows for the investigation of the molecular frame photoelectron angular distributions (MFPADs) of the ionization process. For the photon energies used in this experiment, the Franck-Condon overlap of the H_2 ground state with the energetically accessible part of the $2p\sigma_u$ nuclear wave function is vanishing. Therefore, the photoionization process has long been thought to result in a nuclear wave function of pure gerade parity and a continuum electron wave function of pure ungerade parity. The outcome in this case would be a completely symmetric angular distribution of the photoelectron with respect to the

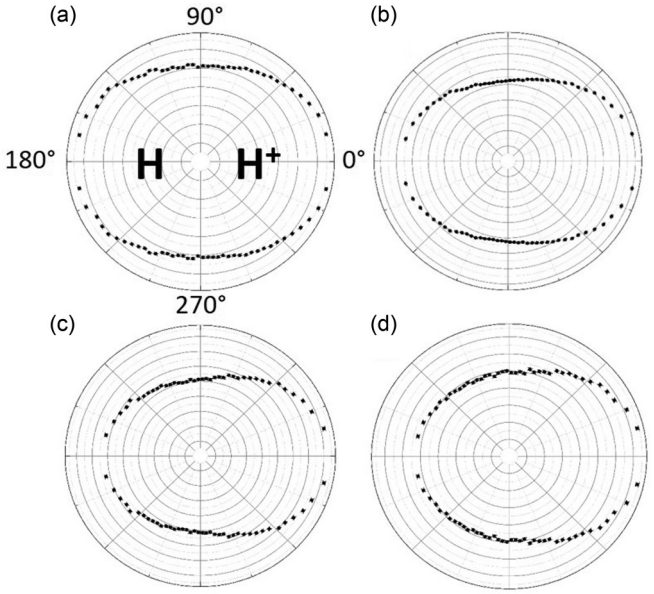

FIG. 3. Polar angular distribution of the ejected photoelectrons in the molecular frame (MFPAD) for the H_2 dissociation channel, where the angle between the electron momentum vector and the molecular axis is shown for KER <0.1 eV and photon energies of 19.8 eV (a), 18.5 eV (b), 18.3 eV (c), and 18.16 eV (d). The statistical error bars are smaller than the symbols. For each histogram, the image is mirrored along the horizontal axis for easier inspection.

charged H^+ and neutral H side of the fragmentation. As shown in the MFPADs of Fig. 3, a striking asymmetry, where the photoelectron is preferentially emitted in the direction of the charged nucleus H^+, is observed.

A theoretical explanation for this effect has been provided by Serov and Kheifets [15], who showed that the retroaction of the Coulomb field of the slow photoelectron onto its dissociating parent ion can lead to a coherent superposition of the nuclear wave functions $1s\sigma_g$ and $2p\sigma_u$ at an internuclear distance R where the two states approach the same energy. For photoelectrons with low kinetic energy, the continuum electron interacts with the dissociating parent molecular ion as the internuclear distance reaches a value sufficient for strong coupling. An efficient coupling to the $2p\sigma_u$ state is expected at an internuclear distance R_c, where the kinetic energies of the nuclei equal approximately the KER value we measure, based on the relationship $U_{2p\sigma_u}(R_c) - U_{2p\sigma_u}(\infty) \approx$ KER, given by Serov and Kheifets [15]. This expectation is confirmed by the increasing asymmetries of the MFPADs with decreasing photon energy. This can be seen in both the former experiment [16] and the present experimental results, shown in Fig. 3. Here, the MFPADs, integrated over all directions of polarization and photon propagation are plotted with a KER limited to be less than 0.1 eV. In both cases, the yield n_{H^+} of electrons emitted along the charged H^+ side of the dissociation increases with decreasing photon energy.

VI. ASYMMETRY PARAMETER

To enable a more quantitative analysis of the dependence of the asymmetry on the electron kinetic energy E_e and kinetic

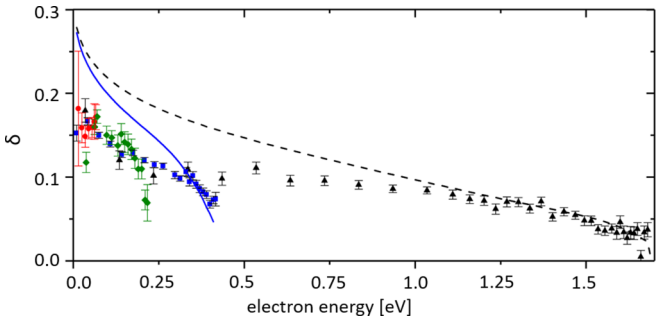

FIG. 4. Asymmetry parameter δ of the dissociation of H_2^+ as a function of the photoelectron energy for photon energies 19.8 eV (black triangles), 18.5 eV (blue squares), 18.3 eV (green diamonds), and 18.16 eV (red circles). The dashed black line shows the classically calculated asymmetry parameter β for 19.8 eV, and the blue solid line shows β for 18.5 eV, with $\beta = 1/\{\pi * [1 + b * r_e(E_e)]\}$, where $b_{19.8\,\mathrm{eV}} = 66.6$ and $b_{18.5\,\mathrm{eV}} = 125$.

energy release KER, we introduce the asymmetry parameter

$$\delta = \frac{n_{H^+} - n_H}{n_{H^+} + n_H}, \tag{5}$$

where n_{H^+} and n_H denote the yield of photoelectrons emitted toward the proton H^+ or opposite toward the hydrogen atom H, respectively. Thus, an asymmetry parameter of $\delta = 0$ corresponds to a symmetric dissociation and $\delta > 0$ to an asymmetric dissociation, with the electron preferentially emerging in the same hemisphere as the ion H^+.

In Fig. 4 the asymmetry parameter δ for H_2 is plotted as a function of the kinetic energy E_e of the photoelectron for photon energies of 19.8, 18.5, 18.3, and 18.16 eV. The general trend in our data is an inverse proportionality of the asymmetry parameter δ to the electron energy E_e, as predicted by Serov and Kheifets [15]. Under closer investigation, one can clearly see deviations from this behavior for the higher electron energies at each photon energy, which corresponds to a KER less than ∼100 meV in each case. In these regions ($E_e = 150$ to 200 meV for a photon energy of 18.3 eV, and 350 to 400 meV for a photon energy of 18.5 eV), the asymmetry parameter δ drops in a linear fashion.

It appears that the asymmetry parameter δ is very sensitive to the photoelectron energy E_e and the kinetic energy release KER of the heavy fragments during the dissociation. We now aim to quantify this relationship. We start by reflecting on symmetry breaking without fields, which has been investigated in detail in the past, and which may provide the basis for a comprehensive theoretical description of the retroaction process and beyond in the future.

VII. ASYMMETRY WITHOUT FIELDS

In general, changes in the asymmetry parameter δ, due to interference between gerade and ungerade states, are expected. The asymmetric electron emission due to the coherent superposition of gerade and ungerade states is known to be highly sensitive to the photoelectron energy and KER, even in the absence of any external or internal fields [15,16]. This becomes more apparent when we take a step back for a moment and consider higher excess energies. Here, we reflect

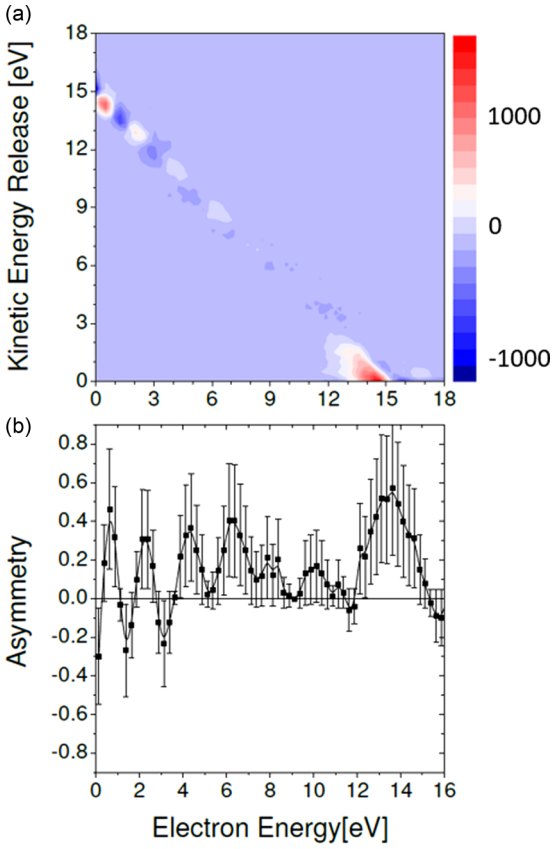

FIG. 5. (a) Asymmetry of the photoelectron emission represented as the yield $(n_{H^+} - n_H)$ in linear color scale of the energy correlation map, spanned by KER as a function of the photoelectron energy E_e for the single ionization and subsequent dissociation of H_2^+ at a photon energy of 33 eV for a Σ to Σ transition (the angle between the light polarization vector and the molecular axis is smaller than 37°). For better visualization of the asymmetry, the difference between the yields along the proton (+) and hydrogen (−) direction $(n_{H^+} - n_H)$ was not normalized to their sum $(n_{H^+} + n_H)$. (b) Projection of the top figure to the electron energy axis for a small slice of the sum energy 14.4 eV $< E_{sum} <$ 16.1 eV, with $E_{sum} = E_e + \mathrm{KER}$.

on the photodissociation of doubly excited (Q2) states of hydrogen molecules with [17] and without [8] external fields, as mentioned in the Introduction.

As an example, in Fig. 5 we plot the asymmetry as the yield of the energy correlation map, spanned by the KER versus the photoelectron kinetic energy E_e for the direct dissociative ionization of H_2 molecules by a single linearly polarized photon with an energy of 33 eV (compare to [17]) in the absence of any internal or external fields. Note that in this case the asymmetry is only the difference between the yields along the proton and hydrogen directions $(n_{H^+} - n_H)$; for visual clarity in this spectrum the difference has not been normalized to the sum of both yields $(n_{H^+} + n_H)$. To grasp the evolution of the asymmetry, we project a thin slice of the distribution 14.4 eV $< E_{sum} <$ 15.1 eV to the electron energy E_e axis in Fig. 5(b). Here, the asymmetry and its evolution are apparent for almost all photoelectron energies due to the interference of resonant photoionization pathways through the $1s\sigma_g$ and

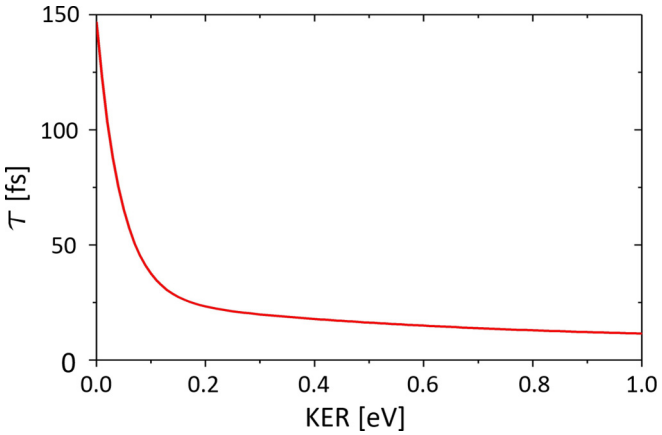

FIG. 6. The dissociation time τ (starting from the mean equilibrium distance of H_2) for the internuclear separation to reach a distance R_c, where the overlap of the $1s\sigma_g$ and $2p\sigma_u$ wave functions is sufficient for interference to be observed as asymmetry in the molecular frame photoelectron distribution.

$2p\sigma_u$ dissociation channels by autoionization decay. It shows linear and sinusoidal regions that could perhaps be accurately described within the Born-Oppenheimer approximation by a state-of-the-art fully quantum mechanical calculation [8].

However, with photon energies ever closer to threshold, at one point electronic and nuclear coupling via Coulomb interactions can no longer be neglected and the Born-Oppenheimer approximation is expected to eventually fail. This near-threshold regime demands a comprehensive quantum mechanical approach including interference effects of gerade and ungerade states depending on the excess energy. To the best of our knowledge, such calculations are not yet available in the energy regime close to threshold, where electronic and nuclear dynamics may not be well described within the Born-Oppenheimer approximation. Despite this, we performed some purely classical estimates of the nuclear and electronic motions for photon energies below 20 eV, in order to explore if the dependence of the asymmetry parameter on the kinetic energy release KER and electron energy E_e can be explained by the kinetics of the particles involved.

VIII. CLASSICAL RETROACTION MODEL

In the following, we return to the investigation of the asymmetry induced by the retroaction mechanism in the molecular dissociation close to threshold. We first calculated the time τ it takes for the dissociating molecule, starting from the H_2 equilibrium coordinate R_e, to reach an internuclear coupling distance of R_c, which corresponds to the KER we measure [15]:

$$U_{2p\sigma_u}(R_c) - U_{2p\sigma_u}(\infty) = \mathrm{KER}. \tag{6}$$

In this step of the calculation we assumed the velocity of the nuclei at any distance R to be given by the energy difference between the $2p\sigma_u$ and the $1s\sigma_g$ potential curves. For small decreasing KER, the modeled dissociation time τ increases very quickly to large values, as can be seen in Fig. 6, where the calculated time τ is plotted as a function of the measured KER. This fast divergence is most rapid just below 100 meV.

In the next step, we estimate the photoelectron distance r_e from the center of mass of the molecule after the dissociation time τ to be

$$r_e(\tau) = \tau\sqrt{2E_e/m_e}. \tag{7}$$

This allows for a simple estimate of the asymmetry parameter, which we call β in the following, in order to distinguish between our measured asymmetry parameter δ. The modeled asymmetry parameter β is expected to scale with the coupling strength of the two states, which is induced through the Coulomb field of the electron ($\sim 1/r_e$). We hence assume the following relation:

$$\beta(r_e) = a/[1 + b * r_e(E_e)]. \tag{8}$$

Here, the factor a is the maximum amplitude of the asymmetry, which is a function of the electron emission θ angle in the molecular frame: $a = \cos(\theta)$. This maximum amplitude is zero for a perpendicular electron emission $\theta = 90^\circ$ and $+1$ for a pinpoint emission toward the proton H^+ with $\theta = 0^\circ$. Since we want to model the positive asymmetry parameters in Fig. 4, we integrate over all electron emission angles, which point into the same direction as the charged fragment H^+. Accordingly, the factor a amounts to $\frac{1}{2\pi}\int_{-\pi}^{\pi}\cos(\theta)d\theta = 1/\pi$. The factor b is a fit parameter, chosen to match our experimental data. In Fig. 4, two examples of the asymmetry parameter β are shown as a function of the photoelectron energy E_e for a photon energy of 18.5 eV (blue solid line) as well as for 19.8 eV (black dashed line). This simple calculation agrees surprisingly well with our experimental data for both energies in the region where the photoelectron energy is higher than the nuclear kinetic energy, i.e., $E_e >$ KER.

The classical model is especially helpful for the interpretation of our experimental data at the extreme ends of the kinetic energies measured in our experiments, i.e., close to zero E_e together with maximum KER and vice versa. As seen in Fig. 6, our calculations of the time τ it takes to reach R_c suggest that the superposition of $1s\sigma_g$ and $2p\sigma_u$ states, which is responsible for the symmetry breaking, occurs on a timescale of ~15–20 fs for kinetic energy releases KERs higher than ~0.1–0.2 eV. This agrees with a time-resolved momentum imaging experiment, measuring the electron localization process in H_2^+ as completed within 15 fs by Xu *et al.* [6]. We would like to stress that even though we did not perform time-resolved measurements in our experiments, we have gained indirect access to the timescale of the dissociation dynamics by measuring and modeling the asymmetry parameter. If the dissociation time τ becomes too large, the photoelectron has moved too far away from the parent molecule to induce a significant coupling. As can be seen in Fig. 6, τ increases rapidly below KER = 0.1 eV. We therefore expect a sudden decrease in the observed asymmetry for dissociations with KER $\lesssim$0.1 eV. As presented in Fig. 4, this appears to be true for the data measured with photon energies of 18.3, 18.5, and 19.8 eV. This trend has not been observed experimentally before. The chosen excess energy, the resolution in KER, and the statistical error bars of Waitz *et al.* [16] are the reasons for no indication of such a change in slope in the previous data set. However, this finding agrees well with the predicted trend by Serov and Kheifets [15], which also shows a sudden decrease in the asymmetry for a KER $\leqslant$0.2 eV.

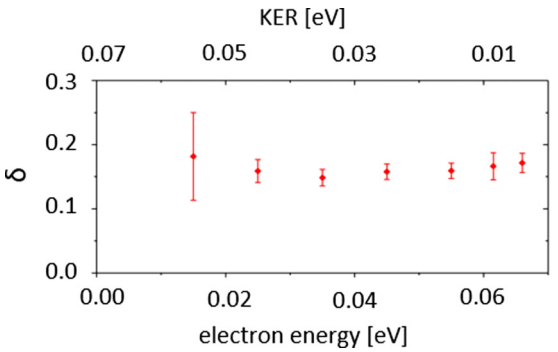

FIG. 7. Asymmetry parameter δ for the dissociation of H_2^+ with $E_\gamma = 18.16$ eV plotted as a function of the electron energy E_e and the kinetic energy release KER. Only contributions from the triplet state with $J = 1$ ($E_{\text{sum}} = 45$ meV) were considered since most of the counts originated from this state [compare the yields of the diagonals with slope -1 in Fig. 2(d)].

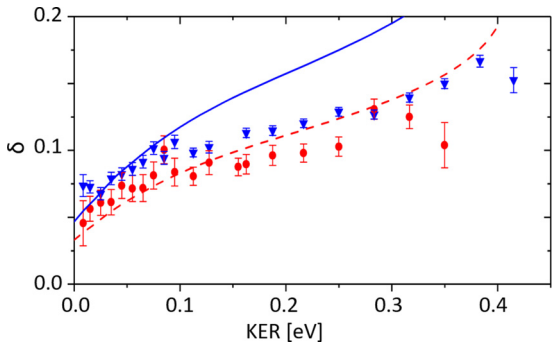

FIG. 8. Asymmetry parameter δ of the dissociation of H_2^+ (blue squares) and D_2^+ (red circles) for a photon energy of $E_\gamma = 18.5$ eV plotted as a function of the KER. The blue solid line shows the result of the classical calculation for the dissociation of H_2^+ using Eq. (8). The dashed red line shows the same, multiplied by the mass scaling factor of $1/\sqrt{2}$.

In the other extreme case, where E_e is very low and the corresponding KER is high, the coupling of electron and nuclear dynamics appears to be on a timescale faster than 15 fs, as seen in Fig. 6. Here, the emitted photoelectron is still close to the molecular cation, and the coupling is accordingly strong. This can also be seen in Fig. 4, where a general increase in the asymmetry parameter is observed for low kinetic energy electrons. The hyperbolic trend of the asymmetry parameter as a function of the electron energy has been predicted by Serov and Kheifets [15] and has been seen by Waitz *et al.* [16] experimentally. However, with ever smaller photon energy the asymmetry parameter appears to saturate in our new data set, which is unexpected. We will elaborate this finding by discussing the results for our lowest photon energy in our measurement sequence as follows.

The dissociative photoionization of H_2 molecules at a photon energy of 18.16 eV shown in Figs. 4 (red circles) and 7 represents a special case. Here, barely above the dissociation threshold, both, electron energy E_e and kinetic energy release KER are below 0.1 eV. Within the statistical error bars of our measured asymmetry parameter δ in Fig. 7, the distribution appears to be flat or perhaps shows an indication of a broad minimum. This trend is not observed at higher photon energies, where we mainly observe a monotonic decrease in the asymmetry with increasing electron energy. In particular, Fig. 7 shows that the asymmetry is strong even on long timescales of the nuclear dynamics, which cannot be explained within our simple classical calculation, modeling the retroaction of the electron. We suspect that the asymmetry parameter δ saturates in our measurements instead of approaching $\delta = 1$. This would be expected for ever lower photon and electron energies, which ultimately would result in a recapture of the photoelectron and a truncation of the ionization process. A possible reason for this saturation lies in the definition of the asymmetry parameter δ in our experiment, which compares the count rate in two half-spheres of the body-fixed electron emission frame, defined in our offline analysis. While further investigation is needed in this energy regime, we believe that a localization beyond the retroaction mechanism is taking place when the electrons and nuclei are both very slow, i.e., approaching similar velocities during the fragmentation process. In this case, the motion of the electrons can no longer be decoupled from the nuclei, and an instantaneous interaction of all particles during ionization takes place, beyond the Born-Oppenheimer approximation. Consequently, the definition of the molecular frame from the final momenta of the three outgoing particles is questionable in this energy regime since the MFPADs in our experimental method ultimately depend on this approximation. A sophisticated theoretical approach would need to account for the complex few-body physics that emerges in this energy regime.

From the discussion above, we do not expect our classical model to be applicable at very low excess energies E_{sum} ($<$100 meV). Therefore, we limit its application to investigate the mass dependency of the asymmetry parameter to a higher photon energy. We chose a photon energy of 18.5 eV to compare the results from the H_2 photodissociation ($\sim$0.425 eV above threshold) with those from the photodissociation of D_2 with the same photon energy ($\sim$0.342 eV above threshold). In Fig. 8, the asymmetry parameter δ of the H_2 and D_2 photodissociation are plotted as a function of the KER. In both cases, the change in slope to an almost linear dependence is found below KER = 0.1 eV. In addition to this, we observe the asymmetry in the D_2 dissociation to be weaker than the H_2 dissociation over the same range of KER. This is to be expected because our classically calculated dissociation time τ is proportional to $\sqrt{m}$, which results in the relationship $\delta \propto 1/\sqrt{m}$, where m is the mass of the atomic fragment. This relation is confirmed well by the calculated parameter β_{H} and $\beta_{\text{D}} = \beta_{\text{H}}/\sqrt{2}$, shown as blue solid and red dashed lines, respectively, in Fig. 8.

IX. SUMMARY

In conclusion, we have performed a detailed investigation of symmetry breaking in the molecular frame photoelectron emission pattern for the dissociative photoionization of diatomic molecules H_2 and D_2. For low photon energies we find that the Coulomb field of the ejected electron couples the electron and nuclear dynamics via retroaction, which is sensitive to the kinetic energies of the particles. By

interrogating a previously unexplored energy regime just above the single-ionization threshold, we present highly differential measurements in MFPADs and asymmetry parameters that are exquisitely sensitive to the coupled electronic and nuclear dynamics. The experimentally observed asymmetry and dynamics as a function of the electron energy E_e, the kinetic energy release KER, and the mass of the nuclei m can be well described classically except for very low excess energies E_{sum} ($<$100 meV), where a more sophisticated treatment appears to be required. In this low-energy regime, the electrons are still about 10 times faster than the nuclei in the dissociation process, but the asymmetry parameter δ shows a noticeable deviation from the classical trend observed $>$100 meV above threshold. This may be a fingerprint of strong electron-nuclei interplay that is beyond the concept of retroaction, and requires a sophisticated model of the instantaneous interaction between all particles during the ionization step, which does not rely on the Born-Oppenheimer approximation. Clearly, further experimental investigations and a better theoretical understanding of this few-body physics is necessary.

To date, quantum mechanical approaches exist to very accurately describe symmetry breaking in the dissociative photoionization of H_2 molecules, in the absence of any fields, such as presented in Fig. 5. Such treatments can serve as the basis and a crosscheck to include nondiagonal matrix elements, in order to push into the regime of non-Born-Oppenheimer behavior in the photodissociation of this fundamentally simple molecule [18]. In best case, such a quantum calculation is able to reproduce the symmetry breaking in H_2 with and without an internal field. The experimental results presented in this paper could serve as benchmarks and stimulate such theoretical investigations to gain a deeper understanding of strong electron-ion interactions during molecular ionization and subsequent dissociation processes.

ACKNOWLEDGMENTS

Work at Lawrence Berkeley National Laboratory was performed under the auspices of the US Department of Energy under Contract No. DE-AC02-05CH11231, and was supported by the US Department of Energy Office of Basic Energy Sciences, Division of Chemical Sciences, Biosciences and Geosciences. This research used resources of the Advanced Light Source (ALS) and the National Energy Research Scientific Computing Center (NERSC), both being US Department of Energy Office of Science User Facilities under Contract No. DE-AC02-05CH11231. We thank the staff of the ALS, in particular at beam line 10.0.1, for their outstanding support. A.G. was financially supported by the ALS through a Doctoral Fellowship in Residence. The J. R. Macdonald Laboratory personnel were supported by the Chemical Sciences, Geosciences, and Biosciences Division, Office of Basic Energy Sciences, Office of Science, US Department of Energy under Award No. DE-FG02-86ER13491. The Frankfurt group acknowledges the support of the Deutsche Akademische Austausch Dienst (DAAD) and the Deutsche Forschungsgemeinschaft (DFG) as part of the DFG research unit FOR1789 as well as the Bundes Ministerium fuer Bildung und Forschung (BMBF). We are indebted to the RoentDek Company for long-term support with detector software and hardware.

[1] M. F. Kling, Ch. Siedschlag, A. J. Verhoef, J. I. Khan, M. Schultze, Th. Uphues, Y. Ni, M. Uiberacker, M. Drescher, F. Krausz, and M. J. J. Vrakking, Control of electron localization in molecular dissociation, Science **312**, 246 (2006).

[2] D. Ray, F. He, S. De, W. Cao, H. Mashiko, P. Ranitovic, K. P. Singh, I. Znakovskaya, U. Thumm, G. G. Paulus, M. F. Kling, I. V. Litvinyuk, and C. L. Cocke, Ion-Energy Dependence of Asymmetric Dissociation of D_2 by a Two-Color Laser Field, Phys. Rev. Lett. **103**, 223201 (2009).

[3] J. Wu, A. Vredenborg, L. Ph. H. Schmidt, T. Jahnke, A. Czasch, and R. Dörner, Comparison of dissociative ionization of H_2, N_2, Ar_2, and CO by elliptically polarized two-color pulses, Phys. Rev. A **87**, 023406 (2013).

[4] Y. Mi, N. Camus, L. Fechner, M. Laux, R. Moshammer, and T. Pfeifer, Electron-Nuclear Coupling through Autoionizing States after Strong-Field Excitation of H_2 Molecules, Phys. Rev. Lett. **118**, 183201 (2017).

[5] G. Sansone, F. Kelkensberg, J. F. Pérez-Torres, F. Morales, M. F. Kling, W. Siu, O. Ghafur, P. Johnsson, M. Swoboda, E. Benedetti, F. Ferrari, F. Lépine, J. L. Sanz-Vicario, S. Zherebtsov, I. Znakovskaya, A. L'huillier, M. Yu Ivanov, M. Nisoli, F. Martín, and M. J. J. Vrakking, Electron localization following attosecond molecular photoionization, Nature (London) **465**, 763 (2010).

[6] H. Xu, Z. Li, F. He, X. Wang, A. Atia-Tul-Noor, D. Kielpinski, R. T. Sang, and I. V. Litvinyuk, Observing electron localization in a dissociating H_2^+ molecule in real time, Nat. Commun. **8**, 15849 (2017).

[7] J. Wu, M. Magrakvelidze, L. P. H. Schmidt, M. Kunitski, T. Pfeifer, M. Schöffler, M. Pitzer, M. Richter, S. Voss, H. Sann, H. Kim, J. Lower, T. Jahnke, A. Czasch, U. Thumm, and R. Dörner, Understanding the role of phase in chemical bond breaking with coincidence angular streaking, Nat. Commun. **4**, 2177 (2013).

[8] F. Martin, J. Fernandez, T. Havermeier, L. Foucar, Th. Weber, K. Kreidi, M. Schoffler, L. Schmidt, T. Jahnke, O. Jagutzki, A. Czasch, E. P. Benis, T. Osipov, A. L. Landers, A. Belkacem, M. H. Prior, H. Schmidt-Böcking, C. L. Cocke, and R. Dörner, Single photon-induced symmetry breaking of H_2 dissociation, Science **315**, 629 (2007).

[9] L. Cattaneo, J. Vos, R. Y. Bello, A. Palacios, S. Heuser, L. Pedrelli, M. Lucchini, C. Cirelli, F. Martín, and U. Keller, Attosecond coupled electron and nuclear dynamics in dissociative ionization of H_2, Nat. Phys. **14**, 733 (2018).

[10] M. P. Bircher, E. Liberatore, N. J. Browning, S. Brickel, C. Hofmann, A. Patoz, O. T. Unke, T. Zimmermann, M. Chergui, P. Hamm, U. Keller, M. Meuwly, H.-J. Woerner, J. Vaníček, and U. Rothlisberger, Nonadiabatic effects in electronic and nuclear dynamics, Struct. Dynam. **4**, 061510 (2017).

[11] R. Dörner, V. Mergel, O. Jagutzki, L. Spielberger, J. Ullrich, R. Moshammer, and H. Schmidt-Böcking, Cold Target Recoil Ion Momentum Spectroscopy: A 'momentum microscope' to view atomic collision dynamics, Phys. Rep. **330**, 95 (2000).

[12] J. Ullrich, R. Moshammer, A. Dorn, R. Dörner, L. Ph. H. Schmidt, and H. Schmidt-Böcking, Recoil-ion and electron momentum spectroscopy: reaction-microscopes, Rep. Prog. Phys. **66**, 1463 (2003).

[13] Y. Hikosaka and J. H. D. Eland, Photoionization into the dissociation continuum of $H_2^+(X^2\Sigma_g^+)$ studied by velocity imaging photoionization coincidence spectroscopy, J. Electron Spectrosc. Relat. Phenom. **133**, 77 (2003).

[14] A. Balakrishnan, V. Smith, and B. P. Stoicheff, Dissociation energies of the hydrogen and deuterium molecules, Phys. Rev. A **49**, 2460 (1994).

[15] V. V. Serov and A. S. Kheifets, *p*-H symmetry breaking in dissociative photoionization of H_2 due to the molecular ion interacting with the ejected electron, Phys. Rev. A **89**, 031402 (2014).

[16] M. Waitz, D. Aslitürk, N. Wechselberger, H. K. Gill, J. Rist, F. Wiegandt, C. Goihl, G. Kastirke, M. Weller, T. Bauer, D. Metz, F. P. Sturm, J. Voigtsberger, S. Zeller, F. Trinter, G. Schiwietz, T. Weber, J. B. Williams, M. S. Schöffler, L. Ph. H. Schmidt *et al.*, Electron Localization in Dissociating H_2^+ by Retroaction of a Photoelectron onto its Source, Phys. Rev. Lett. **116**, 043001 (2016).

[17] A. Fischer, M. Gärttner, P. Cörlin, A. Sperl, M. Schönwald, T. Mizuno, G. Sansone, A. Senftleben, J. Ullrich, B. Feuerstein, T. Pfeifer, and R. Moshammer, Molecular wave-packet dynamics on laser-controlled transition states, Phys. Rev. A **93**, 012507 (2016).

[18] F. Martin and R. Bello (private communication).